Zitierweise: *Angew. Chem. Int. Ed.* **2022,** *61,* e202206831
Internationale Ausgabe: doi.org/10.1002/anie.202206831
Deutsche Ausgabe: doi.org/10.1002/ange.202206831

Dihydrogen Activation

Enhanced Dihydrogen Activation by Mononuclear Iridium(II) Compounds: A Mechanistic Study

*Nereida Hidalgo, Juan José Moreno, Inés García-Rubio, and Jesús Campos**

Dedicated to Maurice Brookhart on the occasion of his 80th birthday

Abstract: The organometallic chemistry of 4d and 5d transition metals has been vastly dominated by closed-shell states. The reactivity of their metalloradical species is though remarkable, albeit yet poorly understood and with limited mechanistic investigations available. In this work we report the synthesis and characterization of two mononuclear Ir^{II} species, including the first dinitrogen adduct. These compounds activate dihydrogen at a dissimilar rate, in the latter case several orders of magnitude faster than its Ir^{I} precursor. A combined experimental/computational investigation to ascertain the mechanism of this transformation in Ir^{II} compounds is reported.

Introduction

Despite its molecular simplicity, dihydrogen (H_2) has captivated chemists for generations. Fundamental, applied, and industrially relevant causes have sustained profound interest and extensive research on its coordination and reactivity.[1] Dihydrogen has been considered the ideal energy carrier,[2] and its efficient complexation and activation is crucial in many areas, including hydrogenation and hydroformylation catalysis, isotopic-labelling reactions or fuel cell applications, among others.[3]

Dihydrogen activation at transition metal centres commonly proceeds through oxidative addition. Heterolytic dihydrogen splitting is also possible and characteristic of the broadening area of metal–ligand cooperation.[4] A common feature of most previous developments in the homogeneous reactivity of H_2 is that they are vastly dominated by diamagnetic species. Contrarily, radical pathways have emerged recently for H_2 activation by main group elements.[5] However, paramagnetic transition metal complexes that bind and split H_2 are yet scarce,[6] albeit their investigation acquires great relevance as it provides the foundation for hydrogen-atom transfer (HAT) reactions.[7] The same applies to the microscopic reverse reaction, namely diamagnetic hydride species that evolve H_2 to produce paramagnetic compounds, for which mechanistic information is very limited.[8]

Group IX diamagnetic metal complexes have played a major role in the fundamental developments and catalytic applications of H_2.[9] On the contrary, paramagnetic mononuclear complexes of Rh^{II},[10] and particularly Ir^{II},[11] are uncommon, and despite recent advances their reactivity remains underexplored. Seminal work from Wayland and co-workers on H_2 splitting by bimetalloradical Rh^{II} porphyrin systems evidenced that the activation of H_2 proceeds in an homolytic fashion characterized by near linear four centred transition states of type $[Rh^{II}\cdots H\cdots H\cdots Rh^{II}]$.[12] Similar homolytic bimetallic pathways were earlier proposed for other metalloradical species.[13] An alternative mechanism was suggested by Reek and van der Vlugt for a mononuclear Rh^{II} complex that is reduced to Rh^{I} via an outer-sphere redox process and then followed by protonation.[14] Metal-ligand cooperation to facilitate heterolytic H_2 splitting over a Rh^{II} site was also suggested by Ozerov,[15] contrasting to a similar Rh^{II} system reported by Milstein for which that possibility was absent, thus revealing no activity towards dihydrogen.[16] More recently, Rauchfuss demonstrated that the metalloradical $[Rh(pyridine)_4(thf)_2]^{2+}$ is an active hydrogen oxidation catalyst, though the H_2 splitting mechanism was not investigated.[17] Related information on iridium(II) species is even more limited. After the seminal examples by Wayland[18] and Wilkinson and Hursthouse (Figure 1),[19] to the best of our knowledge only one other iridium(II) complex capable of activating dihydrogen has been reported, under rather harsh conditions (12 h at 48 bar H_2 and

[*] Dr. N. Hidalgo, Dr. J. J. Moreno, Dr. J. Campos
Instituto de Investigaciones Químicas (IIQ), Departamento de Química Inorgánica and Centro de Innovación en Química Avanzada (ORFEO-CINQA), Consejo Superior de Investigaciones Científicas (CSIC) and Universidad de Sevilla
Avenida Américo Vespucio 49, 41092 Sevilla (Spain)
E-mail: jesus.campos@iiq.csic.es
Dr. I. García-Rubio
Centro Universitario de la Defensa
Ctra de Huesca s/n, 50090 Zaragoza (Spain)
Dr. I. García-Rubio
Department of Condensed Matter Physics,
Faculty of Sciences, University of Zaragoza
Calle Pedro Cerbuna, 50009 Zaragoza (Spain)

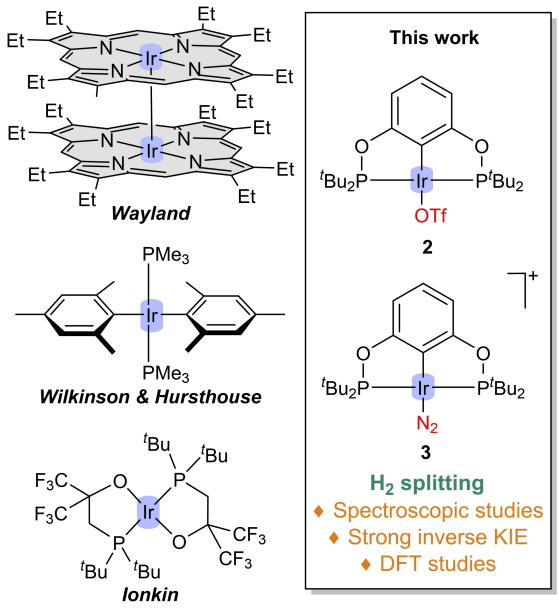

Figure 1. Previous Ir^{II} compounds that split dihydrogen and the ones investigated herein.

70 °C).[20] None of those reports are substantiated by mechanistic studies on the activation of dihydrogen.

In this contribution, we present kinetic, spectroscopic and computational studies of H_2 activation at d^7 Ir^{II} centres. For this purpose, we have synthesized two mononuclear paramagnetic Ir^{II} complexes, Ir(POCOP)OTf (**2**) and [Ir(POCOP)N_2]$BAr^F{}_4$ (**3**) (Figure 1), via oxidation of their Ir^I precursor [Ir(POCOP)N_2] (**1**) with silver salts ((POCOP) = C_6H_3-2,6-$(OP(^tBu)_2)_2$, OTf = trifluoromethanesulfonate, $BAr^F{}_4$ = tetrakis[3,5-bis(trifluoromethyl)phenyl]borate). This work offers the first mechanistic investigation of H_2 splitting at an Ir^{II} complex, which differs from previous suggested pathways in other group IX metalloradicals.

Results and Discussion

The neutral Ir^{II} compound [Ir(POCOP)OTf] (**2**) was synthesized by treatment of the newly prepared [Ir(POCOP)N_2] (**1**) with AgOTf (Scheme 1), which resulted in an instantaneous colour change from orange to green and the appearance of a grey precipitate (Ag); the complex was isolated as a green solid in 93% yield. **2** was silent in $^{31}P\{^1H\}$ NMR spectroscopy,[11e] but a broad signal in the ^1H-NMR spectrum at 16.3 ppm was indicative of a paramagnetic species in solution. On an attempt to isolate an Ir^{II} dinitrogen adduct, we switched to $AgBAr^F{}_4$, anticipating that N_2 coordination would remain in the presence of the weakly coordinating $[BAr^F{}_4]^-$ anion.[21] The reaction of **1** with $AgBAr^F{}_4$ led indeed to a different species (**3**), as hinted by the brown colour of the reaction mixture. Compound **3** was also $^{31}P\{^1H\}$ NMR-silent, though a broad resonance at 4.64 ppm, shifted from that of **2**, was observed by ^1H-NMR.

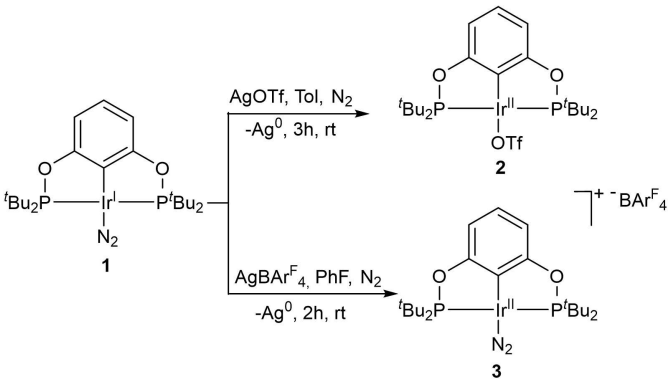

Scheme 1. Synthesis of iridium(II) complexes.

The reaction mixture from which **3** was formed was filtered and single crystals were grown from a saturated benzene solution, enabling the crystallographic determination of its molecular structure (Figure 2).[22] To the best of our knowledge, this constitutes the first example of N_2 coordination to a mononuclear Ir^{II} centre,[23] which duly

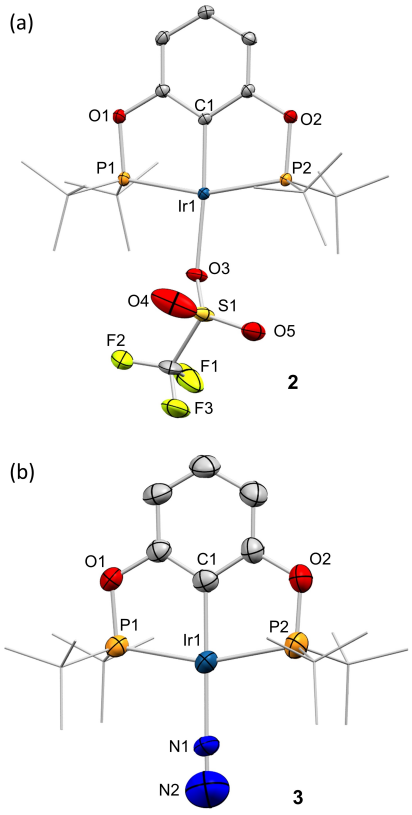

Figure 2. ORTEP diagrams of compound **2** (a) and **3** (b). Hydrogen atoms and the counteranion in **3** are excluded for clarity. Thermal ellipsoids are set at 50% probability. Selected bond lengths [Å] and angles [°]: compound **2**: Ir1–C1 1.969(3), Ir1–P1 2.2932(8), Ir1–P2 2.3092(8), Ir1–O3 2.160(2); P1-Ir1-P2 160.84(3), C1-Ir1-O3 174.83(12), C1-Ir1-P1 80.56(9), C1-Ir1-P2 80.43(9); compound **3**: Ir1–C1 1.979(5), Ir1–P1 2.3133(14), Ir1–P2 2.3160(17), Ir1–N1 2.045(6), N1–N2 1.061 (11); P1-Ir1-P2 160.26(5), C1-Ir1-N1 179.5(3), Ir1-N1-N2 177.4(12), C1-Ir1-P1 80.14(16), C1-Ir1-P2 80.18(16).

adds to the underexplored coordination chemistry of Ir^{II}. The formulation of complexes **1** (Figure S4) and **2** (Figure 2) was confirmed by X-ray diffraction studies as well. These structures exhibit a square-planar geometry, but some striking differences emerge upon oxidation of **1** towards the metalloradical species. The Ir–C bond length decreases in the oxidized compounds (**1**, 2.017(4); **2**, 1.991(5); **3**, 1.979 (5) Å), as foreseen for a stronger σ-donation to the more electrophilic Ir^{II}. However, the Ir–P bond lengths considerably elongate after oxidation (**1**, 2.2764(11), 2.2778(11); **2**, 2.315(1), 2.295(1); **3**, 2.313(1), 2.316(2) Å), an effect that finds precedent in two-coordinate group X complexes and that has been attributed to electrostatic and Pauli repulsion effects rather than to molecular orbital-based reasons.[24] The Ir–N bond length also elongates in **3** (2.045(6) Å) with respect to **1** (1.971(4) Å), while the N–N bond length decreases, likely due to the reduced back-donation to a π*-orbital of N_2 from the oxidized Ir^{II} centre compared to Ir^{I} (d_{NN} = 1.094(6), **1**; 1.061(11) Å, **3**).

Compounds **2** and **3** are one-electron Ir^{II} paramagnets with μ_{eff} = 1.56 and 1.75, respectively, as measured by the Evans method in C_6D_6 (**2**) and C_6H_5F (**3**). Their metalloradical character was further confirmed by EPR spectroscopy that shows a very anisotropic spectrum interpreted as one paramagnetic species with S = 1/2 and g-values 3.95, 1.16 and 0.86 in the case of compound **2** (Figure S19). A different spectrum is found for compound **3** (Figure S20), where two S = 1/2 species with slightly different g-values are detected (3.33, 1.92 and 1.55 vs 3.80, 1.85 and 1.50), which we attribute to the equilibrium between dinuclear and mononuclear dinitrogen species, well-known for related diamagnetic complexes.[25] In addition, their electronic structure was interrogated by means of unrestricted Density Functional Theory (DFT) calculations. The spin density plot of complex **3** (Figure 3) indicates that the iridium oxidation state in the dinitrogen adduct is +2, while for the more electron-rich complex **2** the unpaired electron is delocalized between the metal centre and the phenyl group, suggesting that the formal oxidation state of iridium is somewhat higher than +2.

Our next goal was to analyse the behaviour of **2** and **3** towards H_2. After 7 hours under mild conditions (1 bar H_2, 25 °C), **2** fully converts into the diamagnetic species Ir(POCOP)(H)OTf (**4**)[26] (Scheme 2). Compound **4** exhibits a characteristic hydridic resonance by ^{1}H-NMR at −42.88 ppm, similar to other Ir^{III} POCOP compounds with a vacant site in *trans* disposition to the hydride ligand.[27] Its structure was corroborated by X-ray diffraction studies (Figure S5). Oxidation to Ir^{III} provides a slight elongation of all Ir-containing bonds (ca. 0.05 Å each) with respect to the Ir^{II} compound **2**, while other geometric parameters are comparable to the parent species.

As aforesaid, mechanistic understanding on the homolytic splitting of dihydrogen by Ir^{II} species is lacking, and very limited information for other late-transition metal metalloradicals exists (see literature references cited above). Several mechanistic scenarios can be envisaged for the reaction between **2** and H_2 (Scheme 3): a) Bimetallic homolytic H–H cleavage between 2 equivalents of complex **2**;[6,14,13] b) Outer-sphere H_2 reduction of complex **2** to anionic Ir^{I} and H^+, followed by protonation of the former;[14] c) Formation of a dihydrogen sigma complex and subsequent oxidative addition of the H–H bond to form an Ir^{IV}

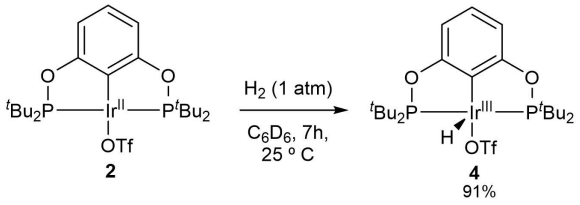

Scheme 2. Reactivity of Ir^{II} complex **2** towards H_2.

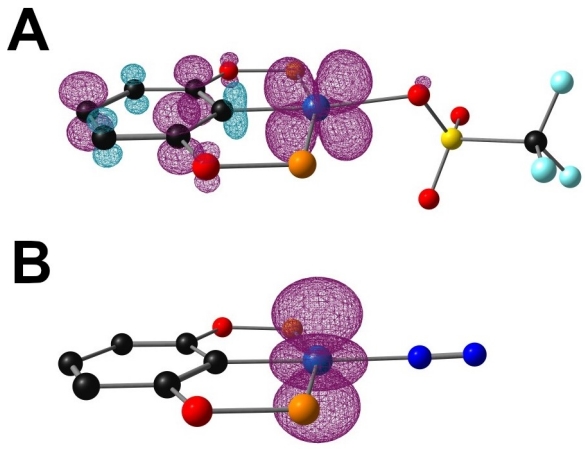

Figure 3. Spin density plot of complexes **2** (A) and **3** (B). H atoms and *tert*-butyl groups were removed for clarity.

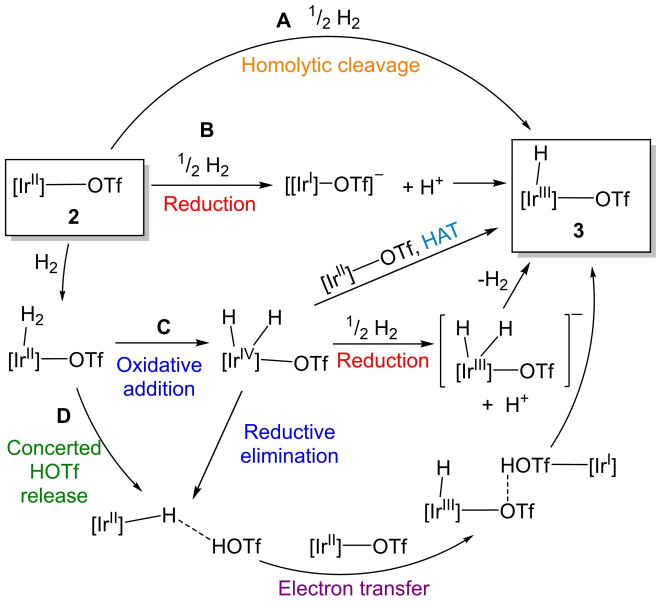

Scheme 3. Mechanistic pathways for hydrogen splitting mediated by **2**. 1/2 has been used as a stoichiometric coefficient.

dihydride, which could be reduced to an anionic Ir^{III} complex by a second equivalent of H_2 and evolved into **4** after hydride abstraction or alternatively being involved in a hydrogen atom transfer (HAT) event with another molecule of **2**;[7] d) Elimination of HOTf from the former σ-H_2 adduct to form an Ir^{II} hydride,[28] which could reduce one equivalent of **2**, forming an ion pair comprised of an Ir^{III} cationic hydride and an Ir^{I} anionic triflate complex, readily reacting with HOTf to give two equivalents of the observed product **4**. We assessed the viability of these pathways by a combined experimental and computational approach.

Monitoring the reaction between **2** and dihydrogen by NMR spectroscopy revealed the presence of starting material **2**, H_2 and the final product **4**. No intermediates were detected in the reaction mixture even at low temperature (−80 °C). The rate of disappearance of **2** under excess dihydrogen (5 bar) followed pseudo-first-order kinetics ($k_{obs} = 0.0170\ s^{-1}$; $\Delta G_{298}^{\neq} = 19.9\ kcal\,mol^{-1}$), suggesting the reaction is first order on the iridium complex **2** (Figure S1). This finding rules out the homolytic bimetallic cleavage pathway (route A in Scheme 3), which is the most commonly invoked route proposed for other metalloradicals,[6,13] in some cases substantiated by second-order kinetics.[12] It also contrasts with the second-order dependence observed by Goldberg for the microscopic reverse process, that is, reductive elimination of dihydrogen from two molecules of an Ir^{III} hydride to form a dinuclear Ir^{II}/Ir^{II} complex.[8a]

A linear dependence of the observed rate constant k_{obs} against the concentration of H_2 at different pressures at 25 °C indicated also a first-order dependence on H_2 concentration (Figure S2). Moreover, the rate constant of the reaction between **2** and D_2 evinced a strong inverse kinetic isotope effect (KIE) of 0.56 ± 0.01. This suggests the involvement of a sigma dihydrogen complex in a rapid equilibrium preceding H–H bond cleavage (routes C and D in Scheme 3),[29] and rules out the direct outer-sphere reduction of complex **2** by H_2 (route B in Scheme 3),[14] for which a normal KIE would be anticipated. Inverse KIEs for H_2 activation reactions remain rare, albeit several examples exist in the literature.[30]

We conducted open-shell DFT calculations to gain further mechanistic insight (Figure 4). The formation of an Ir^{II}-sigma complex is accessible (12.1 kcal mol^{-1} barrier, TS1) and endergonic (5.8 kcal mol^{-1}), in agreement with the lack of experimentally observed intermediates for the reaction. The transition state TS2, found at 20.4 kcal mol^{-1}, displays the attack of an O atom of the triflate group to the metal-bound H_2 moiety, as suggested in route D of Scheme 3, rendering a four coordinate Ir^{II} hydride featuring an interaction with HOTf (Figure S6).[31] Our results indicate that an intermolecular electron transfer between this species and unreacted **2** is highly exergonic (−19.1 kcal mol^{-1}),

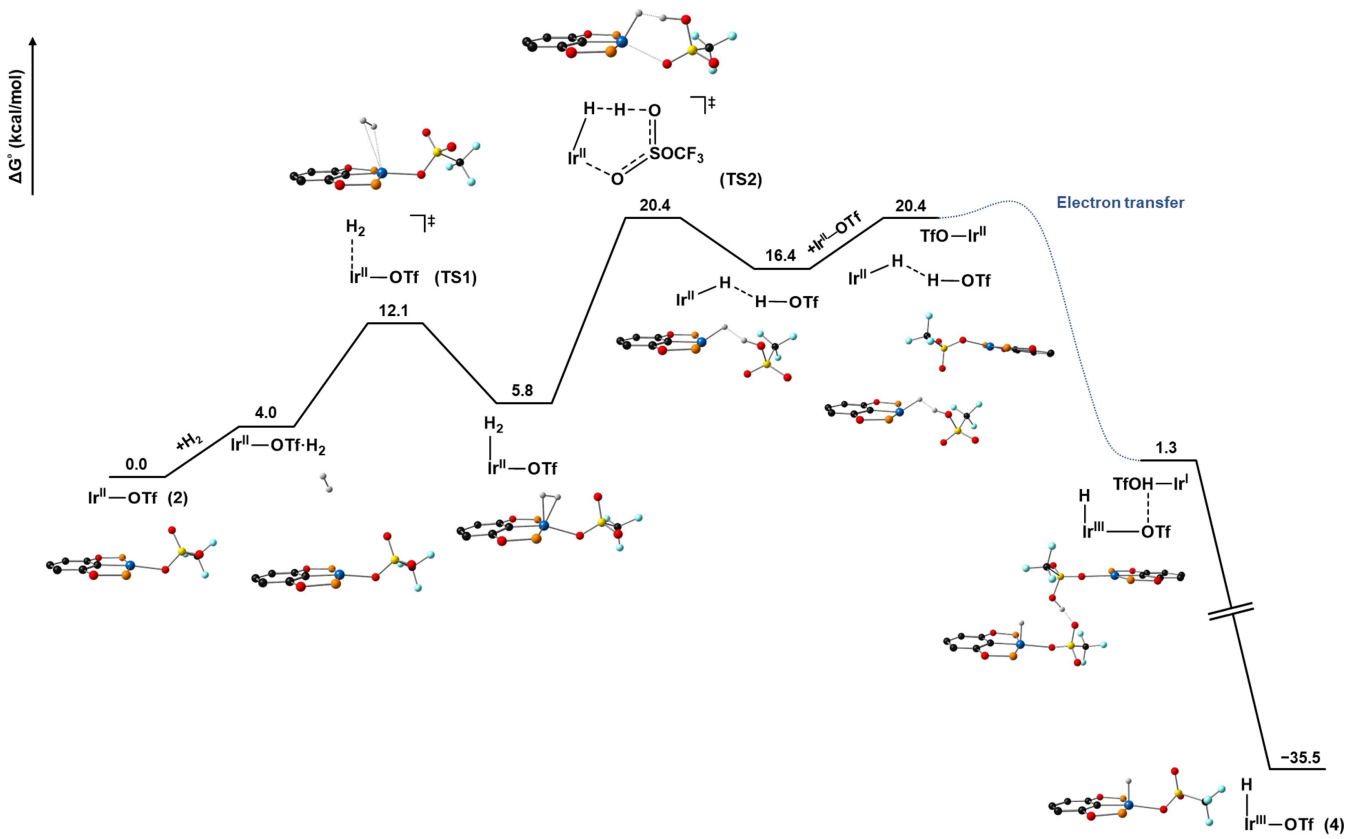

Figure 4. Free energy profile of the proposed reaction mechanism of complex **2** towards H_2 at the PBE0-D3(BJ)/6-311+G(2d,p)//PBE0-D3(BJ)/6-31G(d,p) level of theory.

yielding an ion pair comprised of an Ir^{III} cationic hydride and an anionic Ir^{I} triflate complex. During the geometry optimization of the ion pair with HOTf present, the proton reacts with the anionic unit, rendering a neutral, Ir^{I}-HOTf adduct and an OTf anion that binds to the cationic Ir^{III} hydride, forming one equivalent of **4**. The independent optimization of the Ir^{I}-HOTf adduct likewise evolves to **4** via oxidative addition. To ascertain whether this pathway could explain the experimentally determined inverse KIE, we calculated the KIE for the reaction from the zero-point energy differences ($\Delta\Delta ZPE$) between the reactants, $\mathbf{2}+H_2$, and the H–H bond cleavage TS, to find an inverse KIE of 0.26, in fair qualitative agreement with experiment. The KIE stems from the combination of a 0.22 equilibrium isotope effect (EIE) between **2** and the H_2 sigma complex and a 1.15 KIE from the sigma complex to the H–H bond cleavage TS (Figure S7). Overall, this pathway is in excellent agreement with experimental observations, both by the overall energy and the observed inverse kinetic isotopic effect.

Although the above results are strong support of the mechanism labelled as D in Scheme 3, the aforenamed Ir^{II} σ-H_2 complex, the formation of an Ir^{IV} dihydride is also accessible (9.5 kcal mol^{-1}, TS3) but highly reversible (route C in Scheme 3; Figure S8). A productive transition state for the reductive elimination of HOTf, which would connect this path with the previously discussed one, could not be located. Furthermore, because the redox potential of the $2H^+/H_2$ pair in C_6H_6 is not known and cannot be modelled by DFT methods, further insight on an Ir^{IV}/Ir^{III} H_2-mediated outer-sphere reduction could not be gathered, precluding a complete assessment of the viability of such pathway. Nonetheless, the first-order dependence on the concentration of H_2 seems to disagree with this mechanistic proposal, for which a second-order dependence would be expected.

Finally, a mechanism involving hydrogen atom transfer (HAT) was assessed by computing the bond dissociation free energy (BDFE) of the Ir–H bond in the Ir^{IV} dihydride (18.1 kcal mol^{-1}) and complex **4** (63.7 kcal mol^{-1}). Therefore, while hydrogen atom transfer (HAT) from the Ir^{IV} dihydride to complex **2** is thermochemically accessible, an inner-sphere pathway would present second-order dependence on the concentration of **2**, due to HAT being rate-limiting (the calculated barrier for the formation of the dihydride (9.5 kcal mol^{-1}) is considerably lower than the experimentally determined free energy of activation (19.9 kcal mol^{-1})). Outer sphere HAT from the dihydride presents a calculated barrier of 26.4 kcal mol^{-1}, substantially higher than pathway D. Finally, due to the very low BDFE of the Ir–H bond in the Ir^{IV} dihydride, we considered whether the solvent (C_6H_6) could act as a HAT mediator, which would be consistent with first-order dependence on iridium. Despite HAT to benzene being thermoneutral (BDFE of the C–H bond in the cyclohexadienyl radical (c-C_6H_7) was calculated to be 17.4 kcal mol^{-1}), the lowest-energy transition state for HAT to benzene (TS4, Figure S9) was located above 30 kcal mol^{-1}; quantum tunnelling can be ruled out, as under these conditions it would be accompanied by a large KIE,[32] in stark contrast with the inverse KIE determined for this system. Thus, we also discard this mechanism in favour of the one represented in Figure 4, which is consistent with all our experimental observations.

We also investigated the reactivity of dihydrogen with the Ir^{II} dinitrogen adduct **3** (Scheme 4). In this case, a solution of **3** undergoes immediate colour change from brown to orange-yellow after H_2 addition (1 bar, 25 °C) and two diamagnetic species were observed by NMR in C_6D_6. These complexes were unambiguously assigned to the dihydride and tetrahydride species **5** and **6**, both reported by Brookhart.[33] After 2 hours under H_2 atmosphere complex **6** was the only discernible species (Scheme 4).

The activation of H_2 by compound **3** is considerably more rapid than for the triflate adduct **2**. Even at −80 °C, consumption of **3** was complete in less than 5 minutes, disallowing kinetic experiments alike those carried out for **2**. Because the formation of two new Ir–H bonds in complex **5** is only accompanied by a unitary increase of the Ir oxidation state, it is likely that in this scenario H_2 acts as an outer-sphere reductant. We further supported this hypothesis by carrying out the reaction of **3** and H_2 in the presence of a bulky base that does not bind to the complex, trimesitylphosphine. $^{31}P\{^1H\}$ and ^1H-NMR monitoring confirmed the formation of the corresponding phosphonium cation, formally $[HP(Mes)_3][BAr^F]$. Furthermore, while the reaction of complex **1**, the one-electron reduction product of **3**, with H_2 is sluggish ($t_{1/2}\approx 3.5$ h),[34] in the presence of acid becomes immediate. These data suggest that **3**, much more electrophilic than **2**, could be reduced to Ir^{I} by H_2, producing protons that would facilitate accessing compounds **5** and **6**. The high reactivity the complex exhibits, even at very low temperatures, precludes however a definitive refusal of an alternative Ir^{IV}/Ir^{III} pathway or a bimetallic homolytic cleavage. Nonetheless, this represents an uncommon example in which bond activation is considerably enhanced in the metalloradical Ir^{II} species compared to its reduced Ir^{I} precursor.[17]

Conclusion

In summary, two novel Ir^{II} complexes have been prepared and fully characterized, including the first monometallic Ir^{II} dinitrogen species. The reactivity of these species towards H_2 has been studied by means of a combined experimental

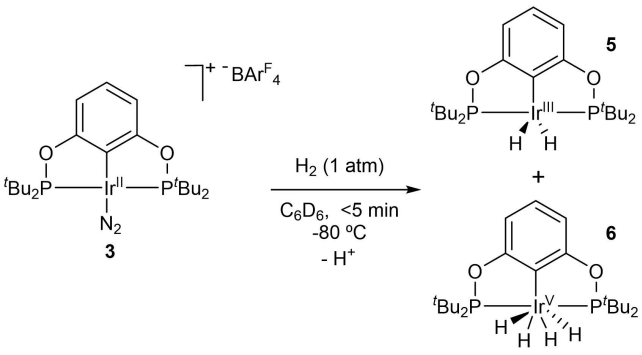

Scheme 4. Reactivity of complex **3** towards H_2.

and computational approach. While for the Ir^{II} triflate complex the reaction rate, reaction orders, and inverse KIE agree with the formation of a sigma complex from which triflate-assisted H–H bond cleavage takes place, for the more electrophilic, cationic Ir^{II}-dinitrogen complex, H_2-mediated reduction of the metal centre is proposed, which is likely followed by the acid-catalysed oxidative addition of H_2. The activation of dihydrogen by the latter Ir^{II} system is remarkably enhanced compared to the conventional Ir^{I} counterpart, evincing the prospects for improved catalytic systems based on unconventional metalloradical species. Overall, these findings notably contribute to the substantially underdeveloped mononuclear Ir^{II} chemistry, for which fundamental mechanistic understanding is yet very limited. Acquiring that fundamental knowledge will be essential for developing innovative bond activation and catalysis based on metalloradical transition metal complexes.

Acknowledgements

This work has been supported by the European Research Council (ERC Starting Grant, CoopCat), the Spanish Ministry of Science (Project PID2019-110856GAI00) and by a PhosAgro/UNESCO/IUPAC research grant in green chemistry. The use of computational facilities at the Supercomputing Centre of Galicia (CESGA) is acknowledged. J.J.M. thanks Junta de Andalucía for the postdoctoral program "Personal Investigador Doctor" (ref. DOC_00153).

Conflict of Interest

The authors declare no conflict of interest.

Data Availability Statement

The data that support the findings of this study are available in the supplementary material of this article.

Keywords: Dihydrogen · Iridium · Metalloradical · Paramagnetic Compounds

[1] a) P. G. Jessop, R. H. Morris, *Coord. Chem. Rev.* **1992**, *121*, 155–284; b) D. M. Heinekey, W. J. Oldham, *Chem. Rev.* **1993**, *93*, 913–926; c) G. J. Kubas, *Chem. Rev.* **2007**, *107*, 4152–4205.
[2] C. Wang, D. Astruc, *Chem. Soc. Rev.* **2021**, *50*, 3437–3484.
[3] R. H. Crabtree, *Chem. Rev.* **2016**, *116*, 8750–8769.
[4] a) B. Askevold, H. W. Roesky, S. Schneider, *ChemCatChem* **2012**, *4*, 307–320; b) O. Eisenstein, R. H. Crabtree, *New J. Chem.* **2013**, *37*, 21–27; c) J. R. Khusnutdinova, D. Milstein, *Angew. Chem. Int. Ed.* **2015**, *54*, 12236–12273; *Angew. Chem.* **2015**, *127*, 12406–12445; d) R. H. Morris Acc, *Chem. Res.* **2015**, *48*, 1494–1502; e) P. A. Dub, J. C. Gordon, *Nat. Chem. Rev.* **2018**, *2*, 396–408; f) M. R. Elsby, R. T. Baker, *Chem. Soc. Rev.* **2020**, *49*, 8933–8987.
[5] E. L. Bennett, E. J. Lawrence, R. J. Blagg, A. S. Mullen, F. MacMillan, A. W. Ehlers, D. J. Scott, J. S. Sapsford, A. E. Ashley, G. G. Wildgoose, J. C. Slootweg, *Angew. Chem. Int. Ed.* **2019**, *58*, 8362–8366; *Angew. Chem.* **2019**, *131*, 8450–8454.
[6] a) D. E. Prokopchuk, G. M. Chambers, E. D. Walter, M. T. Mock, R. M. Bullock, *J. Am. Chem. Soc.* **2019**, *141*, 1871–1876; b) L. R. Doyle, D. J. Scott, P. J. Hill, D. A. X. Fraser, W. K. Myers, A. J. P. White, J. C. Green, A. E. Ashley, *Chem. Sci.* **2018**, *9*, 7362–7369; c) C. Yoo, Y. Lee, *Angew. Chem. Int. Ed.* **2017**, *56*, 9502–9506; *Angew. Chem.* **2017**, *129*, 9630–9634.
[7] J. Choi, Y. Lee, *Angew. Chem. Int. Ed.* **2019**, *58*, 6938–6942; *Angew. Chem.* **2019**, *131*, 7012–7016.
[8] a) J. L. Kuo, K. I. Goldberg, *J. Am. Chem. Soc.* **2020**, *142*, 21439–21449; b) C. K. Blasius, V. Vasilenko, R. Matveeva, H. Wadepohl, L. H. Gade, *Angew. Chem. Int. Ed.* **2020**, *59*, 23010–23014; *Angew. Chem.* **2020**, *132*, 23210–23214; c) C. Rettenmeier, H. Wadepohl, L. H. Gade, *Chem. Eur. J.* **2014**, *20*, 9657–9665; d) D. Inoki, T. Matsumoto, H. Nakai, S. Ogo, *Organometallics* **2012**, *31*, 2996–3001; e) M. B. Chambers, D. A. Kurtz, C. L. Pitman, M. K. Brennaman, A. J. M. Miller, *J. Am. Chem. Soc.* **2016**, *138*, 13509–13512.
[9] See for example: a) R. H. Crabtree, *Acc. Chem. Res.* **1979**, *12*, 331–337; b) E. L. Kolychev, S. Kronig, K. Brandhorst, M. Freytag, P. G. Jones, M. Tamm, *J. Am. Chem. Soc.* **2013**, *135*, 12448–12459; c) R. R. Schrock, J. A. Osborn, *J. Am. Chem. Soc.* **1976**, *98*, 2134–2143; d) L. Vaska, W. DiLuzio, *J. Am. Chem. Soc.* **1962**, *84*, 679–680; e) S. J. Roseblade, A. Pfaltz, *Acc. Chem. Res.* **2007**, *40*, 1402–1411; f) W. J. Kerr, G. J. Knox, L. C. Paterson, *J. Labelled Compd. Radiopharm.* **2020**, *63*, 281–295.
[10] For some recent examples see: a) D. G. DeWit, *Coord. Chem. Rev.* **1996**, *147*, 209–246, and references therein; b) W. I. Dzik, L. F. Arruga, M. A. Siegler, A. L. Spek, J. N. H. Reek, B. de Bruin, *Organometallics* **2011**, *30*, 1902–1913; c) L. Vilella-Arribas, M. García-Melchor, D. Balcells, A. Lledós, J. A. López, S. Sancho, E. Villarroya, P. del Río, M. A. Ciriano, C. Tejel, *Chem. Eur. J.* **2017**, *23*, 5232–5243; d) K. Fuchigami, N. P. Rath, L. M. Mirica, *Inorg. Chem.* **2017**, *56*, 9404–9408.
[11] For some recent examples see: a) K. K. Pandey, *Coord. Chem. Rev.* **1992**, *121*, 1–42, and references therein; b) B. de Bruin, T. P. J. Peters, S. Thewissen, A. N. J. Blok, J. B. M. Wilting, R. de Gelder, J. M. M. Smits, A. W. Gal, *Angew. Chem. Int. Ed.* **2002**, *41*, 2135–2138; *Angew. Chem.* **2002**, *114*, 2239–2242; c) D. G. H. Hetterscheid, M. Klop, R. J. N. A. M. Kicken, J. M. M. Smits, E. J. Reijerse, B. de Bruin, *Chem. Eur. J.* **2007**, *13*, 3386–3405; d) J. Meiners, M. G. Scheibel, M.-H. Lemée-Cailleau, S. A. Mason, M. B. Boeddinghaus, T. F. Fässler, E. Herdtweck, M. M. Khusniyarov, S. Schneider, *Angew. Chem. Int. Ed.* **2011**, *50*, 8184–8187; *Angew. Chem.* **2011**, *123*, 8334–8337; e) Z. Liu, R. J. Deeth, J. S. Butler, A. Habtemarian, M. E. Newton, P. J. Sadler, *Angew. Chem. Int. Ed.* **2013**, *52*, 4194–4197; *Angew. Chem.* **2013**, *125*, 4288–4291.
[12] a) B. B. Wayland, S. Ba, A. E. Sherry, *Inorg. Chem.* **1992**, *31*, 148–150; b) X.-X. Zhang, B. B. Wayland, *J. Am. Chem. Soc.* **1994**, *116*, 7897–7898; c) W. Cui, B. B. Wayland, *J. Am. Chem. Soc.* **2004**, *126*, 8266–8274.
[13] a) J. Halpern, M. Pribanic, *Inorg. Chem.* **1970**, *9*, 2616–2617; b) J. Halpern, *Inorg. Chim. Acta* **1983**, *77*, L105–L106; c) K. B. Capps, A. Bauer, G. Kiss, C. D. Hoff, *J. Organomet. Chem.* **1999**, *586*, 23–30.
[14] J. Wassenaar, B. de Bruin, M. A. Siegler, A. L. Spek, J. N. H. Reek, J. Ivar van der Vlugt, *Chem. Commun.* **2010**, *46*, 1232–1234.
[15] D. E. Smith, D. E. Herbert, J. R. Walensky, O. V. Ozerov, *Organometallics* **2013**, *32*, 2050–2058.
[16] M. Feller, E. Ben-Ari, T. Gupta, L. J. W. Shimon, G. Leitus, Y. Diskin-Posner, L. Weiner, D. Milstein, *Inorg. Chem.* **2007**, *46*, 10479–10490.

[17] Y. Zhang, T. J. Woods, T. B. Rauchfuss, *J. Am. Chem. Soc.* **2021**, *143*, 10065–10069.
[18] K. J. Del Rossi, B. B. Wayland, *J. Chem. Soc. Chem. Commun.* **1986**, 1653–1655.
[19] A. A. Danopoulos, G. Wilkinson, B. Hussain-Bates, M. B. Hursthouse, *J. Chem. Soc. Dalton Trans.* **1992**, 3165–3170.
[20] A. S. Ionkin, W. J. Marshall, *Organometallics* **2004**, *23*, 6031–6041.
[21] I. Krossing, I. Raabe, *Angew. Chem. Int. Ed.* **2004**, *43*, 2066–2090; *Angew. Chem.* **2004**, *116*, 2116–2142.
[22] Deposition Numbers 2123397 (**1**), 2123399 (**2**), 2123398 (**3**) and 2123400 (**4**) contain the supplementary crystallographic data for this paper. These data are provided free of charge by the joint Cambridge Crystallographic Data Centre and Fachinformationszentrum Karlsruhe Access Structures service.
[23] W. Yang, S. Zhang, Y. Ding, L. Shia, Q. Songa, *Chem. Commun.* **2011**, *47*, 5310–5312.
[24] M. C. MacInnis, J. C. DeMott, E. M. Zolnhofer, J. Zhou, K. Meyer, R. P. Hughes, O. V. Ozerov, *Chem* **2016**, *1*, 902–920.
[25] R. Ghosh, M. Kanzelberger, T. J. Emge, G. S. Hall, A. S. Goldman, *Organometallics* **2006**, *25*, 5668–5671.
[26] During the preparation and submission of this manuscript, compound **4** has been reported as a catalyst for the hydrogenolysis of silyl triflates: G. Durin, J.-C. Berthet, E. Nicolas, P. Thuery, T. Cantat, *Organometallics* **2021**, https://doi.org/10.1021/acs.organomet.1c00576.
[27] a) I. Göttker-Schnetmann, P. White, M. Brookhart, *J. Am. Chem. Soc.* **2004**, *126*, 1804–1811; b) I. Göttker-Schnetmann, M. Brookhart, *J. Am. Chem. Soc.* **2004**, *126*, 9330–9338.
[28] This step resembles the widely investigated concerted metalation deprotonation route in the area of C–H bond functionalization. See for instance: a) L. Ackermann, *Chem. Rev.* **2011**, *111*, 1315–134; b) D. L. Davies, S. A. Macgregor, C. L. McMullin, *Chem. Rev.* **2017**, *117*, 8649–8709.
[29] a) D. G. Churchill, K. E. Janak, J. S. Wittenberg, G. Parkin, *J. Am. Chem. Soc.* **2003**, *125*, 1403–1420; b) F. Abu-Hasanayn, K. Krogh-Jespersen, A. S. Goldman, *J. Am. Chem. Soc.* **1993**, *115*, 8019–8023; c) F. Abu-Hasanayn, A. S. Goldman, K. Krogh-Jespersen, *J. Phys. Chem.* **1993**, *97*, 5890–5896; d) G. Parkin, *Acc. Chem. Res.* **2009**, *42*, 315–325; e) B. R. Bender, G. J. Kubas, L. H. Jones, B. I. Swanson, J. Eckert, K. B. Capps, C. D. Hoff, *J. Am. Chem. Soc.* **1997**, *119*, 9179–9190.
[30] a) B. E. Hauger, D. Gusev, K. G. Caulton, *J. Am. Chem. Soc.* **1994**, *116*, 208–214; b) J. M. Camara, T. B. Rauchfuss, *J. Am. Chem. Soc.* **2011**, *133*, 8098–8101; c) N. Hidalgo, J. J. Moreno, M. Pérez-Jiménez, C. Maya, J. López-Serrano, J. Campos, *Chem. Eur. J.* **2020**, *26*, 5982–5993; d) N. Hidalgo, C. Romero-Pérez, C. Maya, I. Fernández, J. Campos, *Organometallics* **2021**, *40*, 1113–1119.
[31] a) S. J. Grabowski, F. Ruipérez, *Phys. Chem. Chem. Phys.* **2016**, *18*, 12810–12818; b) H. Zaher, A. E. Ashley, M. Irwin, A. L. Thompson, M. J. Gutmann, T. Krämera, D. O'Hare, *Chem. Commun.* **2013**, *49*, 9755–9757; c) V. A. Levina, A. Rossin, N. V. Belkova, M. R. Chierotti, L. M. Epstein, O. A. Filippov, R. Gobetto, L. Gonsalvi, A. Lledós, E. S. Shubina, F. Zanobini, M. Peruzzini, *Angew. Chem. Int. Ed.* **2011**, *50*, 1367–1370; *Angew. Chem.* **2011**, *123*, 1403–1406.
[32] T. Hama, H. Ueta, A. Kouchi, N. Watanabe, *Proc. Natl. Acad. Sci. USA* **2015**, *112*, 7438–7443.
[33] I. Göttker-Schnetmann, P. S. White, M. Brookhart, *Organometallics* **2004**, *23*, 1766–1776.
[34] J. M. Goldberg, S. D. T. Cherry, L. M. Guard, W. Kaminsky, K. I. Goldberg, M. Heinekey, *Organometallics* **2016**, *35*, 3546–3556.

Manuscript received: May 10, 2022
Accepted manuscript online: June 23, 2022
Version of record online: July 13, 2022